JMEPEG (2012) 21:1309–1312
DOI: 10.1007/s11665-011-0054-6

1059-9495/$19.00

Effects of Plasma Nitriding on the Tensile Properties of Al-Mg-Si

I.M. Ghauri, R. Ahmad, F.E. Mubarik, Naveed Afzal, Sajjad Ahmed, and R. Ayub

(Submitted April 22, 2011; in revised form August 19, 2011)

Effects of plasma nitriding on the tensile behavior of Al-Mg-Si alloy were investigated in this study. The specimens were nitrided at 70 W input pulsed DC power at 1 mbar pressure of nitrogen for 4 h using glow discharge plasma. The formation of aluminum nitride layer on the specimen's surface was confirmed by the XRD analysis. Stress-strain curves of both un-nitrided and nitrided specimens were obtained using Universal Testing Machine. The comparison of these curves reveals that yield stress, ultimate tensile stress, percentage elongation, and stress relaxation rate decrease after plasma nitriding. The changes in the tensile properties after nitriding have been correlated with the changes in the microstructure of the specimens as observed using scanning electron microscope.

Keywords metals and alloys, microstructure, plasma processing, tensile properties

1. Introduction

Plasma nitriding is a versatile technique which has been widely used for the modification of the surface properties of metals and alloys. In this regard, various efforts in the past have been made to improve the surface hardness of the materials using plasma nitriding. Menthe et al. (Ref 1) investigated the effects of plasma nitriding on the surface hardness of austenite stainless steel in the temperature range of 400-600 °C. The hardness of the specimens was found to increase after plasma nitriding. In another study (Ref 2), it was reported that the plasma nitriding of Al-Mg-Si alloy for various durations and gas pressures increases its hardness. The increase in hardness was attributed to the incorporation of nitrogen into aluminum matrix as an interstitial solid solution. Quast et al. (Ref 3) studied the surface hardness and wear resistance of the pistons made up of commercial aluminum alloys. They observed that the increase in the surface hardness and wear resistance of the alloy is a function of thickness of the nitrided layer. Budzynski et al. (Ref 4) investigated the effects of 120 KeV nitrogen ion implantation on the microhardness of aluminum. The increase of microhardness of the material after ion implantation was attributed to the diffusion of nitrogen ions into the bulk of the material thus resulting in an increase in the internal stresses of the material associated with formation of defects. Influence of nitrogen ion implantation on mechanical properties of low carbon steel was reported by Srivatsan et al. (Ref 5). It was observed that the yield stress decreases and the ultimate tensile stress increases after ion implantation as compared with un-implanted counterparts. The changes in the yielding parameters were rationalized on the basis of free dislocations on the surface, which promote early yielding, and the additional precipitation of nitride particles in the bulk were considered responsible for providing increased strengthening.

From the literature survey, it can be observed that the effects of plasma nitriding on the surface properties of metals and alloys have been the main focus of the research; however, the data available on the bulk properties of nitrided materials are very scarce. The present study has been taken to investigate the effects of plasma nitriding on the tensile properties of Al-Mg-Si alloy.

2. Experimental Work

The material used in the present investigation is the Al-Mg-Si (Al-6061) alloy obtained from Alfa Aesar (USA). The chemical composition of the alloy is given in Table 1. The rectangular strips of 30-mm length, 10-mm width and 1-mm thickness were cut from the as-received sheet. The specimens were first grinded by emery papers of various grade sizes ranging from 250 to 4000 micron and then were fine polished using a diamond paste. The prepared specimens were nitrided in a stainless steel chamber having two circular stainless steel electrodes of diameter 14 cm and a thickness of 2 cm, with an inter-electrode distance of 3 cm (Fig. 1). The chamber was evacuated before the filling of nitrogen gas, using the rotary vane pump. The samples were nitrided in the chamber using a glow discharge plasma at 70 W input pulsed DC power and 1 mbar pressure of nitrogen gas for 4 h. The XRD analysis of the samples was carried out using x-ray diffractometer (Philips Panalytical). The microstructures of both un-nitrided and nitrided samples were examined before and after deformation using Scanning Electron Microscope [JEOL, Japan]. For the tensile tests, the specimens of 10-mm gauge length were fixed in the jaws of universal testing machine. The tensile tests of the specimens were performed at room temperature with a

I.M. Ghauri, Centre for Advanced Studies in Physics, GC University, Lahore, Pakistan; and Centre for Excellence in Solid State Physics, Punjab University, Lahore, Pakistan; **R. Ahmad, F.E. Mubarik, Naveed Afzal, Sajjad Ahmed,** and **R. Ayub**. Centre for Advanced Studies in Physics, GC University, Lahore, Pakistan. Contact e-mail: farrukhehteshamm@gmail.com.

Table 1 Chemical composition of Al-Mg-Si

	Chemical composition, wt.%									
Alloy group	**Mg**	**Si**	**Ti**	**Cr**	**Mn**	**Fe**	**Ni**	**Cu**	**Zn**	**Others**
6061 Al-Mg-Si	0.8-1.2	0.40-0.8	0.15 max	0.04-0.35	0.15 max	0.7 max	0.2	0.15-0.40	0.25 max.	0.15 max.

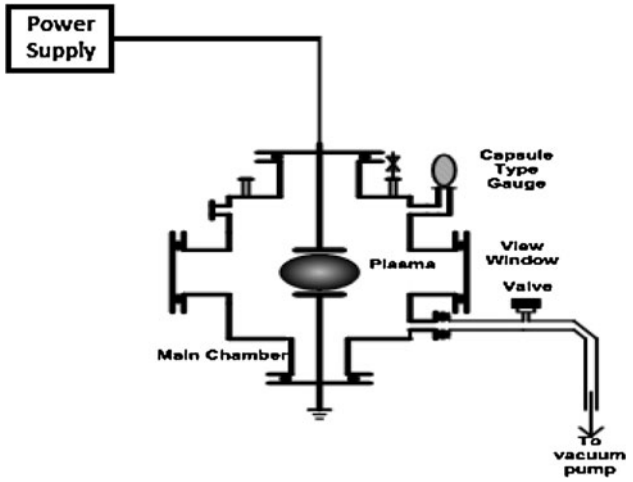

Fig. 1 Schematic diagram of plasma chamber

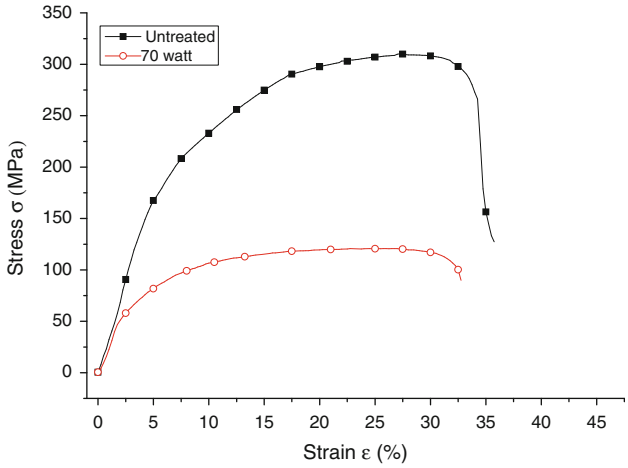

Fig. 2 Stress-strain curves of un-nitrided and nitrided specimen

cross-head speed of 0.5 mm/min. The deformation in the specimens was recorded by the attached computer in the form of stress-strain curves. For the measurement of stress relaxation rate, the cross-head of the machine was interrupted at various stress levels for 60 s, and the amount of stress relaxation with time was recorded. From the analysis of stress-strain curves, the parameters like yield stress, ultimate tensile stress, % elongation, and average value of stress relaxation rate were determined.

3. Results and Discussion

The comparison of stress-strain curves of un-nitrided and those of Al-Mg-Si specimens nitrided at 70 W with 1 mbar nitrogen pressure is shown in Fig. 2. The results show that the yield stress, ultimate tensile stress, and percentage elongation of the specimens decrease after nitriding. Stress relaxation rate in un-nitrided and nitrided specimens was calculated using the relation "$s = d(\Delta\sigma)/d\ \ln(1 + t/t_0)$" (Ref 6). Here $\Delta\sigma$ ($= \sigma_0 - \sigma_t$) is the amount of stress relaxation in time t and t_0 is the small adjustable time which is constant for all the specimens. The variations of stress relaxation rate "s" with stress levels "σ_0" for un-nitrided and nitrided specimens are shown in Fig. 3. It can be observed that the stress relaxation rate increases with increase of stress levels in both un-nitrided and nitrided specimens; however, the relaxation rate has been found to decrease after plasma nitriding.

The XRD results for un-nitrided and nitrided specimens are shown in Fig. 4. The XRD spectrum of un-nitrided specimen shows intense peak at 2θ values of 38.4°, 44.7°, and 65.1° corresponding to (111), (200), and (220) planes, respectively, whereas the XRD analysis of nitrided specimens shows peaks of both aluminum and aluminum nitride at 38.7°, 44.7°, and 65.3°

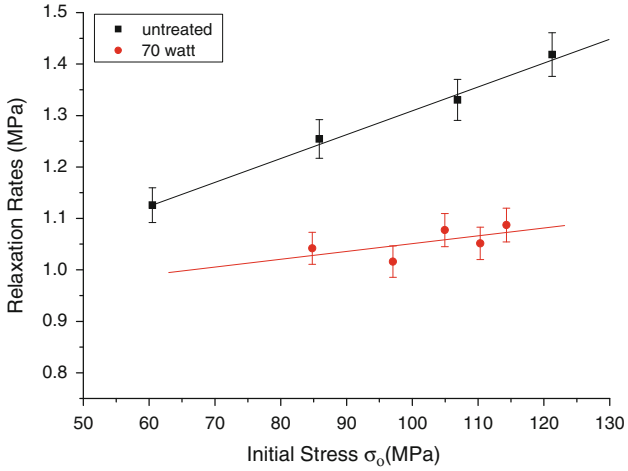

Fig. 3 Variations of stress relaxation rates with initial stress levels for un-nitrided and nitrided specimens

corresponding to (111), (200), and (220) planes, respectively, confirming the formation of aluminum nitride layer on the surface of the specimen. The nitrogen ions react with surface aluminum, thereby forming a layer of aluminum nitride along with aluminum. Nitrogen can also incorporate with the matrix of aluminum interstitially. These incorporations produce stresses at the surface and also change the microstructure of the sample (Ref 7). The microstructral features for un-nitrided and nitrided specimens are shown in Fig. 5. The results show a nodularlike structure of aluminum nitride on the surface of the nitrided specimen. The microstructure of the deformed specimens is shown in Fig. 6.

The decreases in yield stress and ultimate tensile stress of Al-Mg-Si after nitriding may be attributed to the rise of temperature of the specimens during plasma nitriding. As the temperature increases, migration of grain boundaries takes place; finer grains are merged into coarser ones, thus increasing the grain size of Al-6061. The increase in grain size is accompanied by a decrease in the grain boundary area. The dislocations within the grains move during heating process and pile up around the grain boundaries, exerting repulsive forces on the other incident dislocations at the grain boundaries. As grain boundary area decreases, the impediment offered by the grain boundaries to propagating dislocations also decreases, resulting in the reduction of yield and ultimate tensile stresses. The observed decreases of ductility and stress relaxation rate are ascribed to an early generation of cracks in the nitrided specimen (Fig. 6) during deformation. The nitrided specimen behaves as a composite consisting of hard nitride layer and the soft ductile bulk. The hard brittle layer has much higher plastic flow stress than the soft ductile bulk. This difference in stresses generates multi-axial stresses on the surface and within the bulk of the specimen, forcing the soft bulk to contract more in diametrical direction as compared to the nitride layer. Shear stresses are thus generated because of the interaction of transverse stresses acting in the radial direction and the axial stresses acting in the opposite direction. The resultant shear stress is considered to be responsible for the initiation of cracks

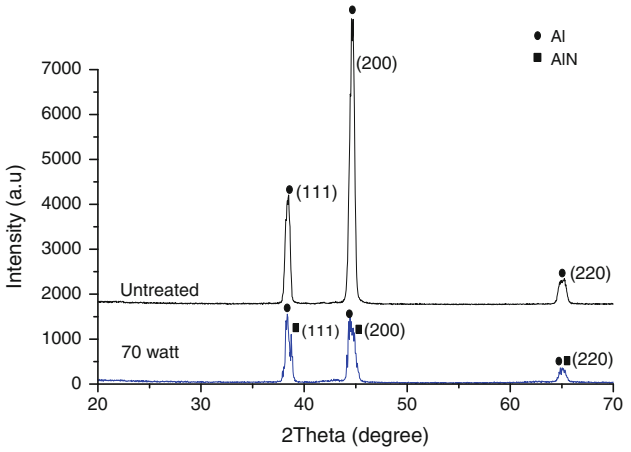

Fig. 4 Comparison of XRD spectra of un-nitrided and nitrided specimen

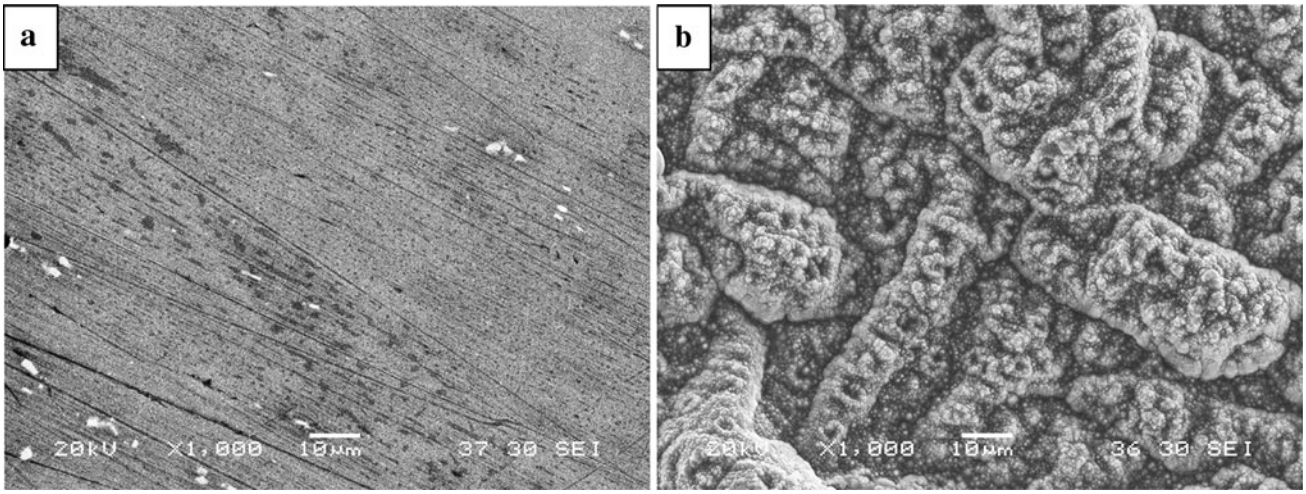

Fig. 5 Microstructures of un-nitrided (a) and nitrided specimens (b)

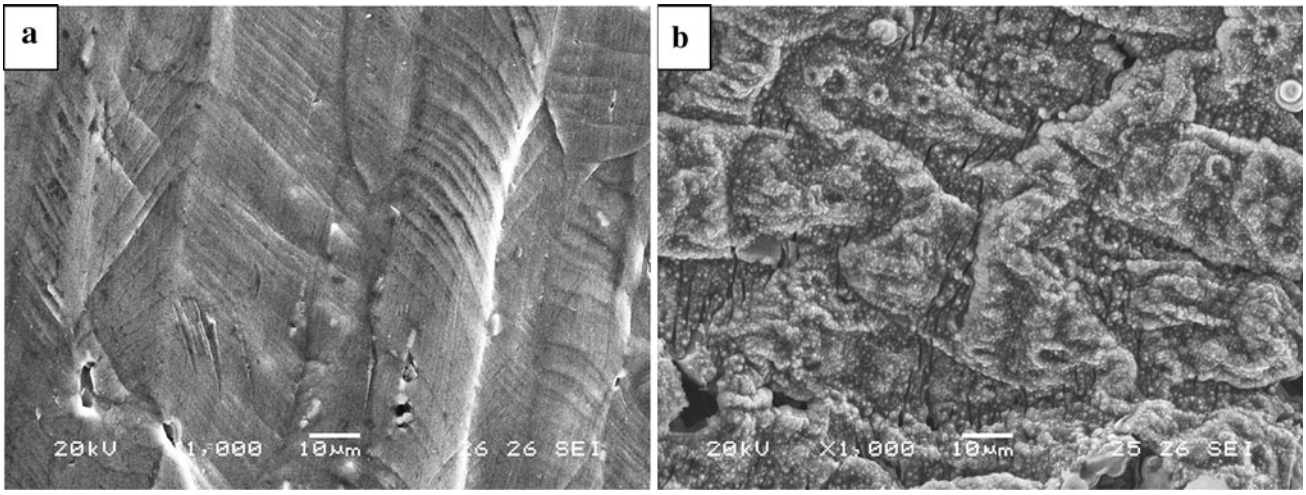

Fig. 6 Microstructures of deformed un-nitrided (a) and nitrided specimens (b)

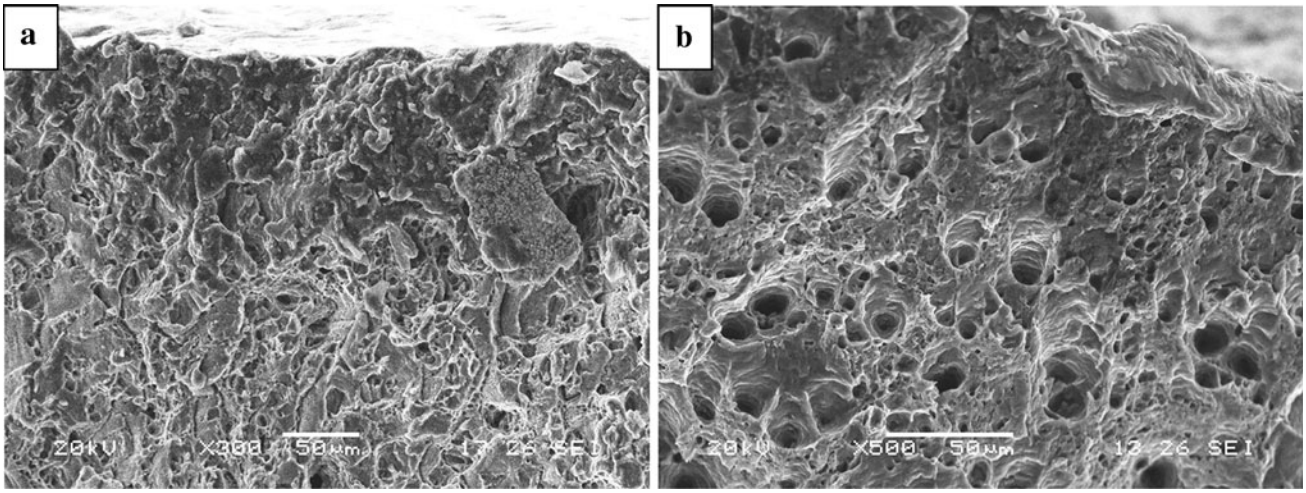

Fig. 7 Fractographs of un-nitrided (a) and nitrided specimen (b)

in the nitrided layer. Once the cracks have been generated, the inner soft bulk does not have the ability to arrest the propagation of the cracks which leads to an early failure of the material (Ref 8). These cracks are also a source of effective impediments during relaxation process. Moreover, the diffusion of nitrogen into the lattice also facilitates the formation of defects in the material. The relaxing dislocations are pinned by these cracks/defects which act as obstacles to their propagation. The enhanced interaction between relaxing dislocations and the defects results in the decrease of stress relaxation rate in nitrided specimen. The comparison of fractographs of un-nitrided and nitrided specimens is shown in Fig. 7. The figure shows that the fracture is moderately brittle and homogeneous, showing platelike features in the case of un-nitrided specimen. However a composite fracture consisting of plate-like facets and dimples is observed for nitrided specimens. The platelike features dominate in the region close to the surface which has became hard and brittle due to nitriding, whereas bulk of the material is full of dimples indicating that fracture here is dominantly ductile.

4. Conclusions

From the present research study, the following conclusions can be drawn.

Plasma nitriding of Al-Mg-Si causes the formation of aluminum nitride layer on the specimen's surface which decreases its yield stress, ultimate tensile stress, percentage elongation, and stress relaxation rate. The stress variations between the bulk and the surface help in the creation of cracks in the nitrided specimen thus resulting into its early failure as compared with the un-nitrided one. Nitriding also facilitates the formation of defects created by the diffusion of nitrogen into the lattice, which results in a decrease of stress relaxation rate in the nitrided specimen.

Acknowledgment

The authors would like to thank Mr. Ahsan Mustaq for his help during the Scanning Electron Microscopy of the Specimens.

References

1. E. Menthe, K.T. Rie, J.W. Schultze, and S. Simson, Structure and Properties of Plasma-Nitrided Stainless Steel, *Surf. Coat. Technol.*, 1995, **74–75**(1), p 412–416
2. M. Shoaib Shah, R. Ahmad, M. Zakaullah, and G. Murtaza, Plasma Characterization for Nitridation of Aluminium Alloy Using 50 Hz AC Discharge, *Plasma Devices Oper.*, 2008, **16**(4), p 247–266
3. M. Quast, H.-R. Stock, and P. Mayr, Plasma-Assisted Nitriding of Aluminum-Alloy Parts, *Met. Sci. Heat Treat.*, 2004, **46**(7–8), p 299–304
4. P. Budzynski, A.A. Youssef, Z. Surowiec, and R. Paluch, Nitrogen Ion Implantation for Improvement of the Mechanical Surface Properties of Aluminum, *Vacuum*, 2007, **81**(10), p 1154–1158
5. T.S. Srivatsan, M. Hanigofsky, T.S. Sudarshan, and K.O. Legg, Influence of Nitrogen Ion Implantation on Tensile Behavior of 1018 Carbon Steel, *Thin Solid Films*, 1992, **213**(1), p 27–33
6. P. Feltham, G. Lehmann, and R. Moisel, Stress Relaxation in Nickel at 20-300 K, *Acta Metall.*, 1969, **17**, p 1305–1309
7. N. Khan, M. Shoaib Shah, and R. Ahmad, Nitriding of Aluminium Alloy in Nitrogen and Nitrogen-Helium Mixture Using 100 Hz-Pulsed DC Glow Discharge, *Plasma Sci. Technol.*, 2010, **12**(4), p 452–460
8. J. Qian, A. Fatemi, and T.S. Cordes, The Influence of Subsurface Nucleation on Uniaxial Fatigue Behaviour of Ion Nitrided Steel, *5th International Conference on Fatigue and Fatigue Thresholds*, Vol 1 (Montreal, Canada), 1993, p 329–334